Trends in Biomaterials and Artificial Organs
www.biomaterials.org.in/tibao
ISSN 0971-1198
https://doi.org/10.5281/zenodo.16957183

Original Article

A Comparative Analysis of the Structural Evolution of Hydroxyapatite Synthesized by Sol-Gel and Microwave-Assisted Methods

Sneha Manoj, Smrithi Saroj, U. Vijayalakshmi*

Department of Chemistry, School of Advanced Sciences, Vellore Institute of Technology, Vellore 632014, India

Received: *3 March 2025*
Accepted: *22 April 2025*
Published online: *26 August 2025*

Keywords: *hydroxyapatite, sol-gel, microwave, crystallite size, sintering*

Several biomaterials have been developed in recent decades for various orthopedic and dental applications with hydroxyapatite (HAP, $Ca_{10}(PO_4)_6(OH)_2$) being an integral one owing to its structural similarity to human bone. Different methods have been explored for the fabrication of HA. Therefore, in this study, we have synthesized HA utilizing two methods namely- refluxing sol-gel and microwave route using the same precursors at different sintering temperatures. A comparative analysis of the phase formation of HA was carried out using XRD, FT-IR, TG-DTA, SEM-EDAX, ^{31}P NMR, and BET analyses. The average crystallite size and degree of crystallinity increased with sintering temperature. FT-IR spectra indicated the presence of carbonate in the sol-gel method and were absent in the microwave method. The weight loss of the samples was observed at 100-400 °C synthesized by both routes. Spherical-shaped particles were formed in sol-gel whereas it was rod-shaped in microwave synthesis. A doublet peak was analyzed in ^{31}P NMR spectra due to the change in the oxidation state of phosphorous and the surface area of the samples was determined by the BET method. Hence, the study proves that different morphological HA can be synthesized through various methods.

Introduction

Hydroxyapatite is one of the important materials that can substitute natural bone in various orthopedic and dental applications. The past few decades have seen an extensive amount of research in hydroxyapatite owing to its unique properties and structural, chemical and biological similarity to the human bone. Hydroxyapatite (HAP, $Ca_{10}(PO_4)_6(OH)_2$) is a thermodynamically stable inorganic compound in different physiological conditions, thus can be used as a suitable bioactive material for various bone graft applications [1]. HAP crystallizes in a hexagonal lattice with a stoichiometric ratio of Ca/P ratio of 1.67. An excellent property required for a biomaterial is biocompatibility which is present in HAP. Moreover, the osteoconductive property (ability to form a bond with natural bone) of HAP make it highly functional to act as a suitable coating on metal implants and helps in bone tissue repair. Therefore, HAP is attracting a huge amount of interest among researchers to study the further modifications achievable in order to enhance its properties [2].

HAP is widely used for various applications as suitable bone grafts and as an effective coating on implants. The biodegradability and bioactivity of HAP is significantly better than nanoparticles making it a more feasible option for biomedical applications. When compared to TiO_2, carbon dots, carbon nanotubes and magnetic particles, HAP is less toxic and more soluble. All these features make HAP a potential candidate for drug delivery applications [3]. Moreover, various ionic substitutions are possible in HAP as calcium, phosphate and hydroxyl groups can be easily replaced by other ions. These substitutions help to improve the properties of HAP such as its poor mechanical strength can be overcome by functionalizing HAP using carbon nanotubes. Similarly, magnetic properties can be imparted to HAP by using magnetic particles which also act as a powerful tool for targeted drug delivery [4].

Different synthesis methods have been employed for the fabrication of hydroxyapatite such as solid-state reaction, co-precipitation, sol-gel, hydrothermal and microwave irradiation [5]. Among these, sol-gel route and microwave assisted technique have received much attention. Sol-gel synthesis have attracted a great deal of interest

* *Coresponding author*
E-mail address: *vijayalakshmi.u@vit.ac.in* (*Dr. Vijayalakshmi U. Department of Chemistry, School of Advanced Sciences, Vellore Institute of Technology, Katpadi, Vellore 632014, Tamil Nadu, India)*

owing to the inherent advantages in the making of glass, ceramic and glass-ceramic powders. The ability to form highly crystalline nanosized particles and thin films, high purity, low synthesis temperature is some of the advantages. Furthermore, molecular-level mixing of the precursors results in a higher degree of chemical homogeneity of the synthesized powders. Additionally, HAP synthesized by sol-gel have shown greater bioactivity due to the presence of ions in the crystal lattice. Metal alkoxides (for eg: tetraethyl orthosilicate for introducing silicon) and metal salts (for eg: calcium nitrate and triethyl phosphate for introducing calcium and phosphorous respectively) are most widely used precursors for the synthesis. Sol-gel is a versatile method for synthesis that helps in the formation of thin film coatings on metal substrates, thereby making HAP highly effective in implant applications [6].

Microwave irradiation is a notable technique which involves the conversion of electromagnetic energy to heat. Uniform transfer of energy is achieved throughout the heating process, therefore enhancing the reproducibility of the synthesis which further improves the yield and purity of the product [7]. This also require less processing time while compared to other methods. It is a cost-effective and eco-friendly process which helps to obtain controlled size, morphology and highly crystalline products. The control of morphology is very important when considered the wide range of applications available to utilize the properties of HAP. Moreover, it provides the synthesis of materials with shorter processing time, lower energy consumption with uniform heating and improved efficacy [8]. The choice of precursors also has a great deal of influence on the various parameters regarding the formation of HAP. As the precursors are changed, it would lead to different reactivity and that can severely impact the processing time and homogeneity of the final product. In general, phosphorous compounds such as phosphoric acid, triethyl phosphite, triethyl phosphate and phosphorous pentoxide are considered for the production of HAP. The proper mode of synthesis along with the suitable precursors can help in the development of nanosized highly crystalline hydroxyapatite [9].

In this investigation, the synthesis of HAP is carried out using two methods: sol-gel and microwave-assisted methods, and then a comparative study is carried out using various characterisation techniques such as XRD and FT-IR. The thermal stability of the samples was analysed by TG-DTA. The structural and morphological studies were done by SEM analysis. The impact of aging time during the sol-gel method was studied using ^{31}P NMR and the specific surface area was determined using BET analysis.

Materials and Methods

Calcium nitrate tetrahydrate [Ca $(NO_3)_2$. $4H_2O$ (99%) SDFCL], triethyl phosphite [$P(OCH_2CH_3)_3$ (98%) Sigma Aldrich] and ethanol [CH_3CH_2OH].

Preparation of HA

Sol-gel method

A refluxing-based sol-gel route was utilized for the fabrication of pure HAP using calcium nitrate and triethyl phosphite as Ca and P resources respectively. First of all, solutions of 0.6 M triethyl phosphite and 1 M calcium nitrate are prepared in ethanol. The stoichiometric ratio of Ca/P is maintained at 1.67 throughout the synthesis. Triethyl phosphite was hydrolyzed by refluxing it at 70°C for 8 hours. The prepared 'Ca' solution was added dropwise to the above refluxed 'P' solution. The solution mixture was again refluxed at 80°C for 16 hrs. This is performed to improve the hydrolyzation and reactivity of the precursors. After that, the sol is evaporated to obtain the gel. The obtained gel is further dried and sintered at 900°C for 2 hrs to obtain powder.

Figure 1: Images of synthesized HAP powder by both the methods

Microwave assisted method

The microwave-assisted synthesis of HAP was carried out using a household microwave oven (IFB) operated under 900W power with a 2.4 GHz frequency. An equal volume of precursor solutions containing 1M of calcium nitrate and 0.6 M of triethyl phosphite were taken and the stoichiometric ratio of Ca/P was maintained at 1.67. The pH was adjusted to 8-10 using aqueous ammonia solution. Then, the prepared solution mixture was kept for magnetic stirring for 2 hrs. After that the resulting mixture was kept inside a microwave oven at continuous heating for 10 minutes. The final product obtained was filtered and washed thrice with distilled water. The calcined powders were obtained after sintering them at 900°C for 2h. The images of the synthesized powders is depicted in figure 1.

Characterization of prepared HAP

The crystallinity of the samples was studied using X-ray diffractometer (XRD, Bruker D8 Advance) using Cu-Kα radiation of 1.5406 Å with 2θ range from 10 to 80°. The thermal analysis of the samples was carried out using Universal V4.5A TA Instruments workstation with a heating rate of 20°C/minute up to 1200°C. The characteristic functional groups for the formation of pure HAP were analysed by Fourier transform infrared spectroscopy with ATR mode (FT-IR: Shimadzu model) in the range 4000 to 400 cm^{-1}. The surface morphology and topography of sintered samples were analysed by Scanning electron microscopy (SEM, Model: Hitachi S4800). All samples were placed on copper sample holders and gold sputtering is carried out to avoid the accumulation of electrostatic charge. The energy dispersive X-ray (EDX) spectra were obtained by a standard unit attached to the SEM. The mechanism of the formation of HAP and the effect of aging time was studied using ^{31}P NMR spectroscopy (Bruker Avance III 400 MHz). The surface area of the powders and the pore size distribution were analyzed (Model: AutosorbiQ, Quantachrome USA). The samples were initially degassed at 150°C for 2 hr and the adsorption/desorption isotherm using nitrogen gas were studied at 300°C. The specific surface area was determined using BET (Brunauer-Emmett-Teller) method.

Results and Discussion

X-Ray Diffraction Studies

X-ray diffraction is an excellent technique to identify the crystalline phases in a sample and to analyze the crystal structure of a particular component. Figure 2(A and B) shows the diffraction patterns

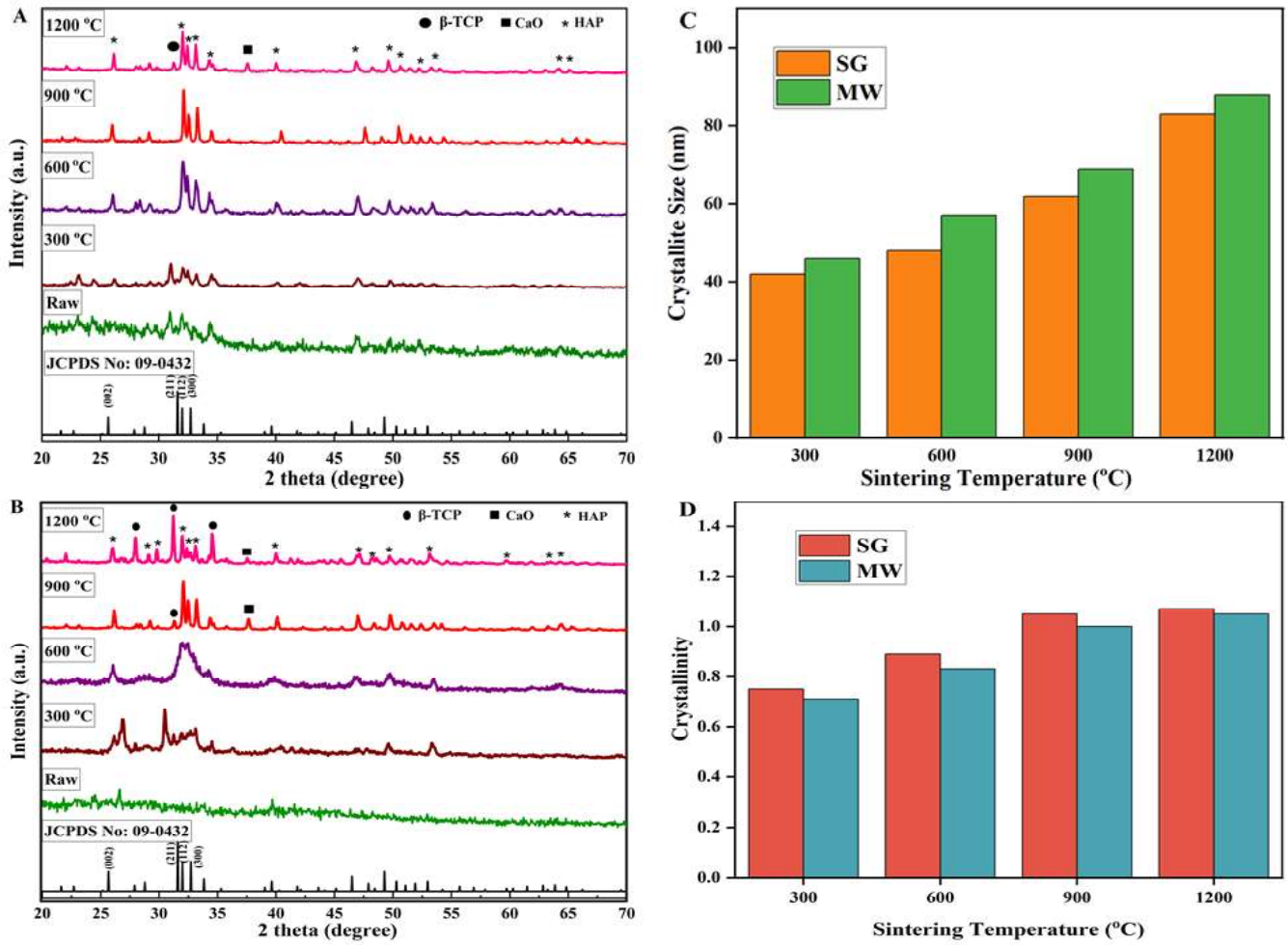

Figure 2: XRD pattern of HAP synthesized by A) sol-gel, B) microwave methods. C) crystallite size and D) crystallinity of HAP at different sintering temperatures

obtained for the HAP samples synthesized by sol-gel and microwave routes respectively. All diffraction peaks obtained exactly matched with the standard pattern of hexagonal structure HAP (JCPDS: 09-432) for both the routes of synthesis. The significant peak positions were observed at 2θ - 25.98°, 31.83°, 32.13°, 32.94° which indicates the major evidence for the formation of HAP [10]. At lower temperatures, amorphous peaks were obtained especially for raw and 300°C sintered samples which accounted for the fact that sintering temperature does affect the crystallinity. At 600°C, when synthesised by sol-gel method, the characteristic peak of HAP was formed with a slight peak broadening which is due to the small amount of amorphous nature present in the sample. But, in the case of the microwave method, a higher degree of amorphous nature was present in the sample as a broad peak was obtained at 600°C. All these findings corroborate the fact that weaker intensity and broadening of the peaks corresponds to the less crystallinity of the material along with the possibility of the formation of nanosized particles. The same can be further proved by calculating the degree of crystallinity (χ_c) using the equation below [11].

$$\chi_c = \left(\frac{0.24\ \text{Å}}{\beta}\right)^3$$

where β is the FWHM (Full Width at Half Maximum) of the particular peak. The peaks became narrower and well-defined at higher sintering temperatures which accounted for the improved crystallinity of the material. Crystallinity improved at higher sintering temperatures due to the growth of the crystal and the decomposition of the carbonate content from the lattice. There is no significant change in the crystallinity from 900 to 1200°C as a majority of carbonate has been eliminated from the lattice below 900°C itself [12]. Crystallization occurs due to the change in the phosphate tetrahedral structure from the amorphous state and the charge is balanced using an anion addition. At higher temperatures, hydroxylated amorphous state is formed by which more charge carriers can be delivered by hydroxyl ions which makes the crystallization easier [13]. The effect of crystallinity and crystallite size of the synthesized HAP at different sintering temperatures is represented in figure 2 (C and D).

At 900°C, in the sol-gel method of synthesis, well-defined highly crystalline HAP is obtained. Similarly, in the microwave-synthesised route, the characteristic HAP was present with a high degree of crystallinity. However, a small amount of β-TCP is also present at 29° for the sample sintered at 900°C, while the presence of β-TCP was seen only at 1200°C in the sol-gel route. Furthermore, the dominant peak in the microwave method at 1200°C is β-TCP along with the less intense HAP. This can be attributed to the fact that β-TCP crystallises at higher temperatures above 1100°C as reported

earlier [14]. Moreover, a small amount of CaO was present when sintered at 1200°C in the sol-gel route, while it is present by 900°C in microwave method and previous reports already suggest that CaO can be present even at 900°C. The presence of CaO at higher temperatures is due to the decomposition of HAP (a) into β-TCP (b) and CaO (c) as expressed below [15].

$$\underset{(a)}{Ca_{10}(PO_4)_6(OH)_2} \rightarrow \underset{(b)}{3Ca_3(PO_4)_2} + \underset{(c)}{CaO} + H_2O$$

The existence of CaO impurity phase reduces the biocompatibility of HAP. This is because CaO dissolves in water to form calcium hydroxide which in turn increases the pH value. This will result in the failure of the implant and obstruct bone formation on the surface of the implant. Hence, it is highly essential to eliminate the secondary phase of CaO. This can be overcome to a greater extent by adding dilute solution of HCl, which converts CaO into $CaCl_2$ and it can be removed by filtration [16]. The presence of the small shoulder peak at 29° also prove that the decomposition of HAP takes place at higher temperatures by the loss of hydroxyl groups and thereby results in the formation of other phosphates. The same phenomenon occurs more significantly in microwave method as the dominant peak at 1200°C is β-TCP [17].

The average crystallite size of the samples was calculated using Scherrer equation:

$$D = \frac{k\lambda}{\beta \cos \theta}$$

where 'D' is the crystallite size, k is the constant and is equal to 0.9, λ is the wavelength of the monochromatic X-ray (1.54 Å), θ is the diffraction angle (°) and β is the FWHM of the peak taken under consideration. The diffraction peak at $2\theta = 26°$ which corresponds to the (002) plane was utilized for the determination of the crystallite size as it is a sharp peak and is isolated from others. The (002) plane shows the growth of the crystal through the c-axis of the HAP crystal structure [18]. It can be seen that as the sintering temperature increased, the peaks became narrower which in turn decreased the FWHM values of the peaks and hence the crystallite size increased. The crystallite size increased from 20 to 40 nm when the temperature increased from 600 to 900°C. Diffusion is the major phenomenon that results in crystallization, hence as the sintering temperature increased, the rate of diffusion of the atoms enhanced which further improves the growth of the crystal and results in larger crystallite size [19].

From the XRD results, it is evident that 800-900°C is the optimum temperature range required to obtain crystalline HAP.

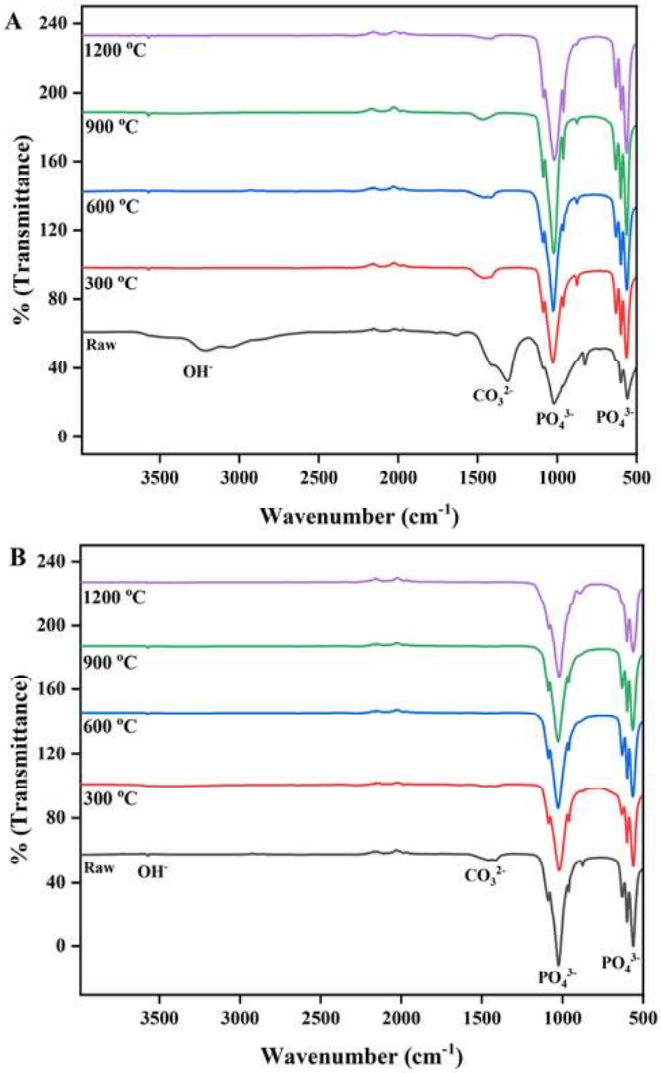

Figure 3: FT-IR spectra of HAP at different temperatures, A) sol-gel route, B) microwave method

FT-IR Analysis

The FT-IR spectroscopy was used to detect the characteristic functional groups present in the samples. Figure 3 (A and B) represents the FT-IR spectra of the samples synthesized by sol-gel and microwave methods sintered at different temperatures respectively. The characteristic chemical groups of HAP which includes PO_4^{3-}, OH^- and CO_3^{2-} were present in all the samples. The tetrahedral symmetry of HAP produces four different vibrational modes namely- symmetrical stretching vibrational mode at 960 cm^{-1} (non-degenerated mode, ν_1), doubly degenerated bending vibrational mode at 460 cm^{-1} (ν_2), asymmetrical stretching triply degenerated vibrational mode at 1010-1130 cm^{-1} (ν_3) and triply degenerated bending vibrational mode at 550-600 cm^{-1} (ν_4). These modes of phosphate group were present in all the samples which confirms the structure of HAP [20].

HAP consist of two types of OH^- groups which corresponds to the two different types of water present. One is present in the apatite structure and its characteristic bending and stretching vibrational bands are present at 630 and 3570 cm^{-1}respectively. For the raw sample a broad peak is seen which becomes narrower on increasing the sintering temperature which is a characteristic feature of HAP. It indicates a higher degree of crystallinity at higher temperatures which was also evidenced by XRD results. The other one is lattice water which consist of a broad band region in the range of 1600 and 3300-3500 cm^{-1}. At higher temperatures, dehydration occurs due to heating and the intensity of these bands diminishes and gets eliminated. The presence of hydroxyl group can be seen when synthesised by both the routes [21].

The band present at 1470 cm^{-1} is associated with stretching vibrational mode and the band at 860 cm^{-1} belongs to the bending vibrational mode of CO_3^{2-} group respectively. When synthesised by sol-gel method, a highly intense carbonate peak is obtained at 1470 cm^{-1} for the raw sample which might be due to the interaction with carbon dioxide present in atmosphere. The intensity of the peak decreased with higher sintering temperature as carbon dioxide

is a volatile gas and hence gets easily eliminated [22]. In the microwave method of synthesis, only a small shoulder peak of carbonate is present for the raw sample as the synthesis is taking place in a closed environment with a short duration of time (10 min) which reduces the possibility of the interaction with carbon dioxide. The intensity of the peak drastically reduced and vanishes at higher temperatures. Hence, it can be proved that carbonated apatite can be produced using sol-gel technique while compared to the microwave method. Carbonated apatite is more applicable for orthopaedic applications as human bone contains small amount of carbonate and helps in improving the osteoconductive potential of HAP [23].

Thermal analysis

Thermo gravimetric analysis (TGA) provides information regarding the weight loss of the powders whereas differential thermal analysis (DTA) provides details of the type of reaction the raw samples undergo with an increase in temperature. The thermal stability of HAP raw powder is illustrated in figure 4A, when synthesised by sol-gel method. The figure depicts a weight loss of 30 % between 0 to 200°C which corresponds to the loss of adsorbed water. The same is also reflected with the presence of a sharp endothermic peak in DTA curve at the same region. During thermal treatment, HAP go through two main processes which include dehydration and dihydroxylation [24]. Dehydration is the removal of adsorbed water which takes place at less than 200°C and the same can be corroborated from FT-IR spectra also as no band of adsorbed water is visible at 300°C and higher. Dihydroxylation is the removal of structured water which takes place between 250 to 600°C and the same can be evidenced by the IR spectra as the hydroxyl peaks gets narrower at higher temperatures. After 600°C no significant weight loss is observed which prove the greater stability of HAP at temperatures 700°C and above [25].

In the microwave method also (figure 4B), the weight loss of the raw HAP is similar to the TGA curve of the sol-gel method. An endothermic peak at about 600°C was observed due to the formation of apatite from other phosphates. No other significant change was observed in the samples when treated at higher temperatures.

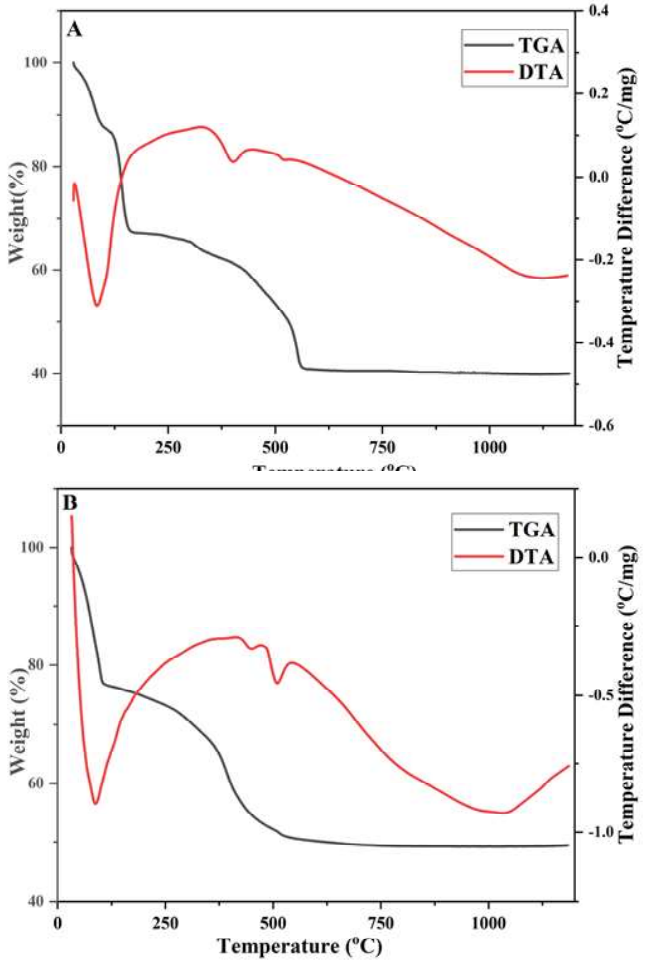

Figure 4: TGA and DTA curve of raw HAP powder, A) sol-gel and B) microwave route

^{31}P NMR spectroscopy

The possible mechanism of the formation of HAP when synthesised by sol-gel can be analysed using ^{31}P NMR (figure 5). Sol-gel method consist of two main processes which include hydrolysis and polycondensation. Hydrolysis is the step that is carried out to improve the dispersion ability of the precursor in the solution. Hence, triethyl phosphite reacts with ethanol to form diethyl phosphate. The alkoxide ligands (-OR) gets protonated as a result of hydrolysis followed by the subsequent elimination of the charged ligand (-OR+) culminating in the nucleophilic addition of negatively charged hydroxyl group to the positively charged 'P' (reactions a) and b)) [26]. This will then act as the pronounced site for the addition of Ca ions and finally 'sol' is formed. The final step is the polycondensation of the 'sol' which occurs by evaporation and results in the formation of intermediate Ca-O-P bonds. Finally, 'gel' is formed which is then heated to obtain the powder. The same mechanism can be explained using NMR spectra. In the figure, it can be seen that non-hydrolyzed 'P' has only one peak which corresponds to the oxidation state of 'P' which is +3. Upon hydrolysis, triethyl phosphite (a) changes to diethyl phosphate (b) and the oxidation state increases to +5. This is represented in the equation 1 provided below. The same can be observed in the spectra as a doublet peak is present at -0.5 and -2.2 ppm. After the addition of the Ca ions, the 'sol' is aged for 16 hours and the spectrum is analyzed. We can see that on interaction with calcium nitrate (d), a Ca-O-P bond is formed and the peaks gets shifted to the -more negative region as the aging time increases, which implies the shielding effect. It is because diethyl phosphate forms a chelating complex (e) with calcium (equation 2) and thus the apatite structure is formed [27].

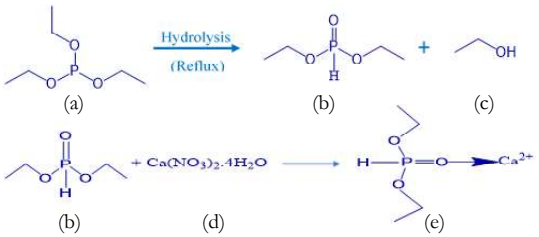

SEM analysis

Scanning Electron Microscopy is used to obtain the morphological characteristics of the samples. Fig. 6 shows the SEM micrographs of the samples. The samples sintered at 900 °C were taken for the analysis. When synthesised by sol-gel, spherical round-shaped morphology was found for the particles. The particles were also agglomerated non-uniformly. Various parameters such as aging time and addition time play an important role in deciding the shape of the particles. It has been reported that quick addition of

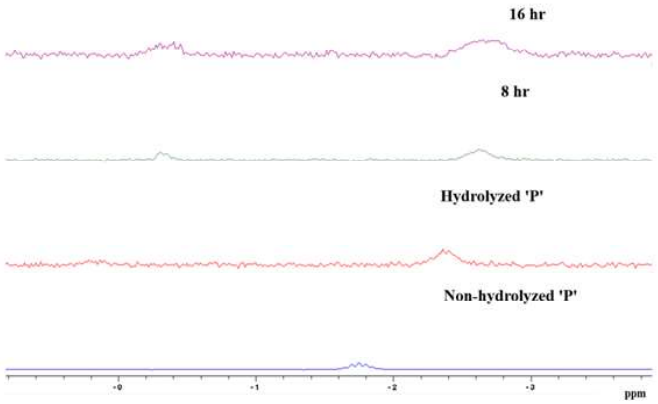

Figure 5: Effect of aging time in sol-gel synthesis depicted by ^{31}P NMR spectroscopy

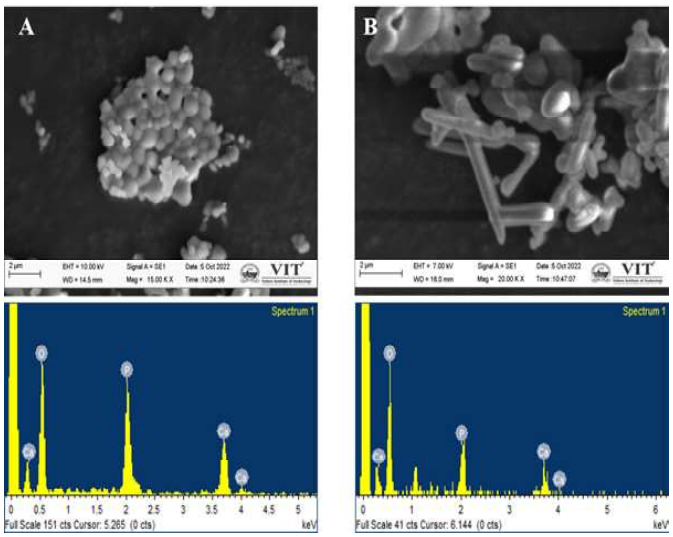

Figure 6: SEM and EDAX images of A) sol-gel derived HAP, B) microwave derived HAP

phosphorous precursor into the ethanolic solution of $Ca(NO_3)_2$ helps in the formation of a spherical shape [28]. In the case of microwave method of synthesis, rod-shaped morphology was found which clearly indicates that the shape can be controlled by changing the synthesis conditions. The size and shape also influence the osteoblast proliferation and osteogenic potential in biocompatibility evaluation. According to the findings by Turk et.al., rod-like shaped nanoparticles show a decreased osteoblast proliferation which results in the failure of the material to act as a suitable coating on implants. When the shape of the particles is spherical, more osteogenic expression is observed, making them suitable for various applications [29]. Increasing the duration of the synthesis time can bring changes to the morphology of the particles. This is because nucleation and growth of the crystals take place dynamically due to fast oscillation of ions in the solution, making only a part of the crystal to grow, thus the formation of nanorods [30].

The corresponding EDAX spectra was also obtained for the samples which confirmed the presence of Ca, P, O elements. The Ca/P ratio of both the samples were found to be in the range of 1.65 ~ 1.66 which was approximately equal to the stoichiometric ratio of biological apatite (1.67).

BET analysis

The porosity characteristics such as specific surface area and pore size are important parameters that determine the effectiveness of a suitable biomaterial. The 900°C sintered powders were taken for analysis. The nitrogen adsorption/desorption isotherms of HAP synthesised by both the methods were shown in figure 7. A type IV isotherm with a typical hysteresis loop is present which arises due to capillary condensation, thereby specifying the presence of a mesoporous structure (2-50 nm) [31]. The specific surface area increased from 17.5 to 22.8 m^2g^{-1} for microwave and sol-gel synthesis routes respectively. Microwave irradiation causes aggregation of particles which decreases the surface area. Also, as the synthesis time increases, consolidation of more particles take place due to continuous microwave treatment which also contributes to the increase in the surface area [32]. A sharp increase in the range of 0.99 P/P_0 suggest a broader pore size distribution (figure 6B). In the case of sol-gel method, a wider pore size distribution in the range of 20 nm was found, whereas pore size distribution was in the range of 35 nm in the case of microwave method. Higher surface area results in smaller pore size as they

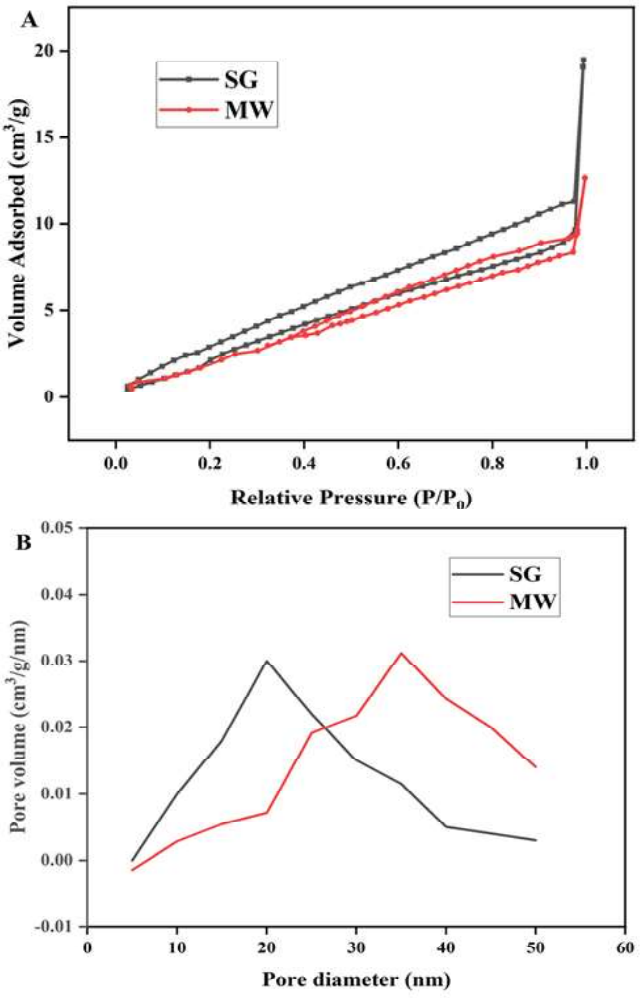

Figure 7: A) BET adsorption/desorption isotherm of HAP, B) pore-size distribution of HAP

follow an inverse relationship with each other. Higher surface area can help in introducing more active sites in HAP which in turn helps in improving its potential as suitable drug carriers for various applications [33]. In our future research, we aim to develop HAP coatings on titanium implant by spin-coating method followed by drug loading on HAP for various biomedical applications.

Conclusion

The synthesis of HAP was carried out successfully using both sol-gel and microwave methods, which helps to obtain phase pure crystals. Carbonated apatite was formed using sol-gel route whereas no substitution was present in the microwave method. Carbonate content is more beneficial for various applications, thereby making sol-gel a feasible method for HAP production. CaO, the secondary phase usually formed which also hinder its biocompatibility can be eliminated through refluxing sol-gel synthesis as it is only present at very high temperature. Another advantage of using sol-gel method is that it does not require the need of any special equipment unlike microwave method. HAP synthesised by both methods were also found to be thermally stable at elevated temperatures. Spherical and rod-shaped morphology were observed by SEM micrographs. Thus, it can be concluded that even though HAP can be synthesized by microwave and sol-gel routes, refluxing based sol-gel method provide far more advantages that is necessary for improving the potential of HAP as a suitable coating material on implants and as a drug carrier for bone regeneration applications.

Acknowledgement

The authors thank VIT, Vellore for providing the necessary support and facilities to perform the research activities. One of the authors highly acknowledge the VIT SEED Grant (File No: SG20220035) for the financial support.

References

1. S. Ramesh, C. Y. Tan, R. Tolouei, M. Amiriyan, J. Purbolaksono, I. Sopyan, W. D. Teng, Sintering behavior of hydroxyapatite prepared from different routes, Mater. Des., 34, 148-154 (2012).
2. P. Kumar, B.S. Dehiya, A. Sindhu, Bioceramics for hard tissue engineering applications: A review, Int. J. Appl. Eng. Res., 13(5), 2744-2752 (2018).
3. S. A. X. Stango, U. Vijayalakshmi, Synthesis and characterization of hydroxyapatite/carboxylic acid functionalized MWCNTS composites and its triple layer coatings for biomedical applications. Ceram. Int., 45(1), 69-81 (2019).
4. R. Zhao, P. Xie, K. Zhang, Z. Tang, X. Chen, X. Zhu, Y. Fan, X. Yang, X. Zhang, Selective effect of hydroxyapatite nanoparticles on osteoporotic and healthy bone formation correlates with intracellular calcium homeostasis regulation, Acta Biomater., 59, 338-350 (2017).
5. S. A. X. Stango, U. Vijayalakshmi, In vitro electrodeposition of hydroxyapatite coatings on Ti-6AL-4V for biomedical applications, Int. J. Chem. Tech. Res., 7, 958 (2015).
6. B. Priyadarshini, U. Vijayalakshmi, Preparation and characterization of sol-gel derived Ce 4+ doped hydroxyapatite and its in vitro biological evaluations for orthopedic applications. Mater.Des., (2017).
7. M. N. Hassan, M. M. Mahmoud, A. Abd El-Fattah, S. Kandil, Microwave-assisted preparation of Nano-hydroxyapatite for bone substitutes, Ceram. Int., 42(3), 3725- 3744 (2016).
8. B. Priyadarshini, U. Vijayalakshmi, Development of cerium and silicon co-doped hydroxyapatite nanopowder and its in vitro biological studies for bone regeneration applications, Adv. Powder Technol., 29(11), 2792-2803 (2018).
9. M. A. Nazeer, E. Yilgor, M. B. Yagci, U. Unal, I. Yilgor, Effect of reaction solvent on hydroxyapatite synthesis in sol–gel process, Royal Soc. Open Sci., 4(12), 171098 (2017).
10. L. Guo, M. Huang, X. Zhang, Effects of sintering temperature on structure of hydroxyapatite studied with Rietveld method, J. Mater. Sci: Mater. Med., 14, 817-822 (2003).
11. O. Kaygili, S. V. Dorozhkin, T. Ates, A. A. Al-Ghamdi, F. Yakuphanoglu, Dielectric properties of Fe doped hydroxyapatite prepared by sol–gel method, Ceram. Int., 40(7), 9395-9402 (2014).
12. M. U. Jahangir, F. Islam, S. Y. Wong, R. A. Jahan, M. A. Matin, X. Li, M. T. Arafat, Comparative analysis and antibacterial properties of thermally sintered apatites with varied processing conditions, J. Am. Ceram. Soc., 104(2), 1023-1039 (2021).
13. S. Waheed, M. Sultan, T. Jamil, T. Hussain, Comparative analysis of hydroxyapatite synthesized by sol-gel, ultrasonication and microwave assisted technique, Materials Today: Proceedings, 2(10), 5477-5484 (2015).
14. U. Vijayalakshmi, S. Rajeswari, Influence of calcium precursors on the morphology and crystallinity of sol-gel derived hydroxyapatite nanoparticles, J. Cryst. Growth, 310(21), 4601-4611 (2008).
15. H. Eshtiagh-Hosseini, M. R. Housaindokht, M. Chahkandi, Effects of parameters of sol–gel process on the phase evolution of sol–gel-derived hydroxyapatite, Mater. Chem. Phys., 106(2-3), 310-316 (2007).
16. M. F. Hsieh, L. H. Perng, T. S. Chin, H. G. Perng, Phase purity of sol–gel-derived hydroxyapatite ceramic, Biomater., 22(19), 2601-2607 (2001).
17. A. Costescu, I. Pasuk, F. Ungureanu, A. Dinischiotu, M. Costache, F. Huneau, S. Galaup, P. L. Coustumer, D. Predoi, Physico-chemical properties of nano-sized hexagonal hydroxyapatite powder synthesized by sol-gel, Dig. J. Nanomater. Biostruct., 5(4) (2010).
18. Y. X. Pang, X. Bao, Influence of temperature, ripening time and calcination on the morphology and crystallinity of hydroxyapatite nanoparticles, J. Eur. Ceram. Soc., 23(10), 1697-1704 (2003).
19. S. C. Wu, H. C. Hsu, S. K. Hsu, C. P. Tseng, W. F. Ho, Effects of calcination on synthesis of hydroxyapatite derived from oyster shell powders, J. Aust. Ceram. Soc., 55, 1051-1058 (2019).
20. M. Safarzadeh, C. F. Chee, S. Ramesh, M. A. Fauzi, Effect of sintering temperature on the morphology, crystallinity and mechanical properties of carbonated hydroxyapatite (CHA), Ceram. Int., 46(17), 26784-26789 (2020).
21. G. Muralithran, S. Ramesh, The effects of sintering temperature on the properties of hydroxyapatite, Ceram. Int., 26(2), 221-230 (2000).
22. C. Kothapalli, M. Wei, A. Vasiliev, M. T. Shaw, Influence of temperature and concentration on the sintering behavior and mechanical properties of hydroxyapatite, Acta. Mater., 52(19), 5655-5663 (2004).
23. L. Berzina-Cimdina, N. Borodajenko, Research of calcium phosphates using Fourier transform infrared spectroscopy in *Infrared Spectroscopy-Materials Science, Engineering and Technology*, 12(7) 251-263 (2012).
24. M. Trzaskowska, V. Vivcharenko, A. Przekora, The impact of hydroxyapatite sintering temperature on its microstructural, mechanical, and biological properties, Int. J. Mol. Sci., 24(6), 5083 (2023).
25. J. Zhou, X. Zhang, J. Chen, S. Zeng, K. De Groot, High temperature characteristics of synthetic hydroxyapatite, J. Mater. Sci. Mater. Med., 4, 83-85 (1993).
26. U. Vijayalakshmi, S. Rajeswari, Influence of process parameters on the sol-gel synthesis of nano hydroxyapatite using various phosphorous precursors, J. Sol-Gel Sci.Technol., 63, 45-55 (2012).
27. K. A. Gross, C. S. Chai, G. S. K. Kannangara, B. Ben-Nissan, L. Hanley, Thin hydroxyapatite coatings via sol–gel synthesis, J. Mater. Sci.: Mater. Med., 9, 839-843 (1998).
28. J. A. Lett, K. Ravichandran, and M. Sundareswari, The study on the synthetic methodologies for manoeuvring the morphology crystallinity and particle size of hydroxyapatite, J. Chem. Pharm. Res., 7(2), 231-239 (2015).
29. S. Türk, Ý. Altýnsoy, G. ÇelebiEfe, M. Ýpek, M. Özacar, C. Bindal, Microwave– assisted biomimetic synthesis of hydroxyapatite using different sources of calcium, Mater. Sci. Eng., C, 76, 528-535 (2017).
30. Y. Z. Wang Y. Fu, Microwave-hydrothermal synthesis and characterization of hydroxyapatite nanocrystallites, Mater. Lett., 65, (23-24), 3388-3390 (2011).
31. A. Huang, H. Dai, X. Wu, Z. Zhao, Y. Wu, Synthesis and characterization of mesoporous hydroxyapatite powder by microemulsion technique, J. Mater. Res. Technol., 8(3), 3158-3166 (2019).
32. W. Amer, K. Abdelouahdi, H. R. Ramananarivo, M. Zahouily, A. Fihri, K. Djessas,
K. Zahouily, R. S. Varma, A. Solhy, Microwave-assisted synthesis of mesoporous nano-hydroxyapatite using surfactant templates, Cryst. Eng. Comm., 16(4), 543-549 (2014).
33. A. A. Sery, H. A. El-Boraey, S. A. Abo-Elenein, R. M. ElKorashey, CuFe2O4@ hydroxyapatite composite for the environmental remediation of some heavy metal ions: Synthesis and characterization, Water Sci., 35(1), 154-164 (2021).